

Influence of Filtering upon Precision and Trueness in Conoscopic Holography

David Blanco, Pedro Fernández, Pablo Zapico, Natalia Beltrán and Carlos Suárez

Abstract—3D digitizing techniques are capable for providing a huge amount of data to represent a particular surface. In reverse engineering tasks it is a common procedure to apply filters that remove singular points in order to obtain lighter and easier-to-handle point-clouds. Nevertheless, election of filtering parameters and cut-off values is an important question, since it could be affecting reliability of measurements. In this work, an analysis of filtering influence upon precision and trueness in conoscopic holography digitizing is presented. Results suggest that no simultaneous optimization can be performed upon both quality indicators, whereas a filtering strategy focused on optimizing standard deviation of measurements could help for improving quality of digitizing.

Index Terms—Conoscopic holography, repeatability, trueness

I. INTRODUCTION

CONOSCOPIC holography (CH) is an interferometric technique first described by Sirat and Psaltis [1] and patented by Optimet Optical Metrology Ltd. This technique calculates the distance between a source of laser light and an object by analysing the diffraction pattern generated by the laser beam when it passes through a conoscopic crystal after being reflected by object surface. In latter work, Sirat et al. [2] have pointed out some CH advantages upon more-popular Laser Triangulation techniques. Better repeatability, capacity for digitizing high-sloped surfaces or a higher robustness under variable surface conditions are among these advantages. CH sensors have been incorporated in industrial developments by Álvarez et al. [3] among others. Nevertheless, a huge variety of applications, going from roughness measurement to dimensional inspection, defects detection or soft-tissues scanning have been reported [4] - [8].

Like other optical digitizing techniques, CH is affected by surface properties, and sensor configuration parameters have to be adjusted depending on surface material and

characteristics to provide reliable measurements. CH sensors have two main configuration parameters: *power* (P) and *frequency* (F). Thus, the amount of energy emitted by the sensor is controlled by P , and the exposure ratio is controlled by F . A proper values selection for these parameters is crucial in order to improve the quality of the digitized point-cloud.

Signal-to-Noise Ratio (SNR) is commonly accepted as the main quality indicator although, in fact, it just only reflects signal quality. Other quality indicators, as *Total* (an indicator that is proportional to the area limited by signal envelope) have to be considered according to the manufacturer recommendations. In a recent work, Fernández et al. [9] have pointed out a series of recommendations for a proper selection of P and F values. The number of valid points and the distribution of errors within the working range (WR) of the sensor are among the indicators that should have to be considered according to their work.

Nevertheless, attention has to be paid to the fact that a proper configuration of digitizing parameters should lead to a really dense point-cloud. If this is the case, the operator should explore the possibilities of applying filters to reduce the weight of the digitized data without significantly modifying reconstruction quality.

Subsequently, filtering strategies may become an important task and some decisions have to be taken in order to select adequate filters and to establish proper cut-off filtering values. Though CH filtering necessity has been previously mentioned by [6] and [10], no systematic analysis of filtering conditions and how they are influencing the overall accuracy of the system has been developed up to date.

II. EXPERIMENTAL FRAMEWORK

A. Objective

The main objective of present work is to analyse the influence of filtering design upon precision and trueness of measurements calculated using conoscopic-holography-digitized 3D data.

B. Factors

Three filtering alternatives have been considered in this work: *SNR*, *Total* and *Outliers*. As it has been explained before, *SNR* provides information about the quality of the signal used for establishing the distance between the sensor and the surface. High values for *SNR* indicate high signal quality. Manufacturer recommends a minimum 500 *SNR* value (in a 0 to 1023 range) for an adequate signal reconstruction. *Total*, on the other hand, represents the

Manuscript received 14 March, 2014; revised 24 March, 2014. This work was supported by the Spanish Ministry of Economy and Competitiveness and FEDER (DPI2012-30987) and the Regional Ministry of Economy and Employment of the Principality of Asturias (Spain) (SV-PA-13-ECOEMP-15).

D. Blanco is a Full Time Lecturer (e-mail: dbf@uniovi.es).

P. Fernández is a Lecturer (e-mail: pedrofa@uniovi.es).

P. Zapico is a Research fellow (e-mail: pablozapicog@gmail.com).

N. Beltran is an Associated Lecturer (e-mail: nataliabeltran@uniovi.es)

C. Suarez is a Professor (e-mail: csuarez@uniovi.es).

The corresponding address for all authors is: Department of Manufacturing Engineering, University of Oviedo, Campus de Gijón, 33203 Gijón, SPAIN.

amount of energy that is collected by the sensor. Although manufactures recommends values of *Total* within the range from 1,200 to 16,000, there is not an optimal value recommendation on this parameter. Finally, in present work, *Outliers* have been defined as those points with spatial positions that are relatively distant from the average position of the whole point cloud representing a particular surface. *Outliers* are often related to transient malfunctions on the measuring system or to physical causes like located abnormal surface properties (brightness, shining, colour...). The cut-off distance for identifying and removing outliers has been therefore considered in this work.

C. Quality Indicators

Distance between parallel planes *d* has been selected as the main quality indicator in present work. Precision is defined as the closeness of agreement between independent test results obtained under stipulated conditions. In this work, precision is expressed in terms of repeatability, and the standard deviation for *d* has been thereafter considered. Following this, σ_d represents the standard deviation of a series of values calculated for the distance between parallel surfaces obtained from point clouds that have been digitized under the same scanning conditions within a short period of time. Trueness, on the other hand, is defined as the difference between the average value of a certain parameter obtained from a large series of test results and an accepted reference value. Following this, δ_d represents the difference between a reference (assumed as true) value *D* and the average values of *d* obtained from *j* consecutive scanning runs denoted as \bar{d}_j (1).

$$\delta_d = D - \bar{d}_j \quad (1)$$

D. Materials and Methods

A stepped stainless steel part (AISI 316), obtained by wire EDM machining, has been used as test specimen. Two flat surfaces with a theoretical distance of 4 mm have been selected and their correspondent digitized point-clouds have been used for calculating quality indicators.

All measurements within this work were conducted using a DEA Swift Coordinate Measurement Machine (CMM) which Maximum Permissible Linear Measuring Tolerance (MPE_E) and Maximum Permissible Probing Tolerance (MPE_P) were certified as in (2 and 3).

$$MPE_E = 4 + 4 \cdot 10^{-3} \cdot L [\mu m], \text{ being } L \text{ in mm} \quad (2)$$

$$MPE_P = 4 [\mu m] \quad (3)$$

Conoscopic measurements were obtained using an Optimet Conoprobe Mark 10 sensor mounted on the CMM (Fig. 1). Calibration procedure of the measuring system was realised using the methodology developed in previous works [11]. The sensor was equipped with a 50 mm focal length lens, which provides an 8 mm wide working range (WR). Main characteristics of this sensor can be found on Table I.

TABLE I
CHARACTERISTICS OF CONOPROBE MARK 10 SENSOR

Property	Value
Measuring speed	9000 Hz
WR (50 mm lens)	8 mm
Stand-off (50 mm lens)	44 mm
Precision* (50 mm lens)	5 μm
Repeatability 3 σ (50 mm lens)	1 μm
Angular coverage	170°

Finally, to provide an appropriate reference value, *D* has been calculated using a contact measurement touching probe with the same CMM. Twenty points were captured on each plane, and distance between planes was therefore calculated. This procedure was repeated 15 times, so that *D* was defined as the average of distance values.

A specially-designed fixture has been used to locate and orientate the specimen within sensors WR. This fixture has levelling screws that allow for an accurate orientation of both test surfaces parallel to CMM XY plane. Using this system, test surfaces were located so that they stand at a 2 mm nominal distance from the theoretical stand-off distance. This means that the upper surface was be located in a +2 mm plane with respect to the stand-off, whereas the lower surface was located in a -2 mm plane. According to this, both surfaces are equally-distanced from the optimal digitizing point. An image of the CMM during test specimen digitizing can be found on Fig. 1.



Fig. 1. Conoscopic holography digitizing of test specimen.

III. PRELIMINARY TESTS

Prior to define the design of experiments, a series of preliminary test were carried out to properly delimitate experimental conditions. *P* and *F* values were selected following [9]. After recommended values were adapted to the Mark 10 specifications, a (P2000; F3000) configuration was established for all the experimental runs within this work.

The two surfaces were digitized once to obtain a preliminary description of *SNR* and *Total* distribution.

Additionally, each point-cloud has been processed and a best-fit plane has been calculated. Afterwards, orthogonal distances between every single point and correspondent best-fit plane have been obtained.

Results indicated that *SNR* values distribution presents a strong dependence with distance to the sensor. Furthermore, no overlapping can be observed between *SNR* distributions for both planes (Fig. 2 and Fig. 3).

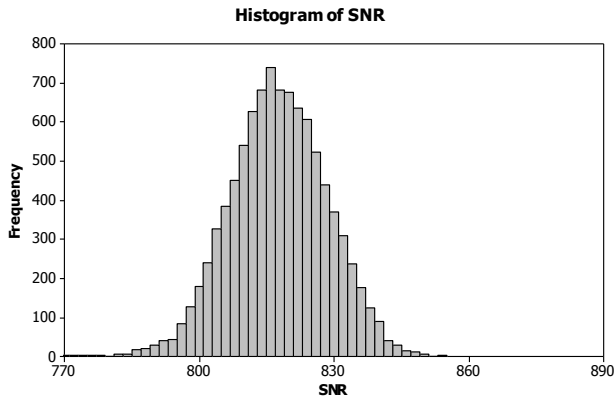


Fig. 2. Histogram of *SNR* distribution for the lower (-2 mm) surface.

Maximum *SNR* values for the lower plane do not exceed 850, whereas minimum *SNR* values within the upper plane are always higher than 850. Consequently, if a common *SNR* filter range would be applied to both point-clouds simultaneously, asymmetric results would be expected.

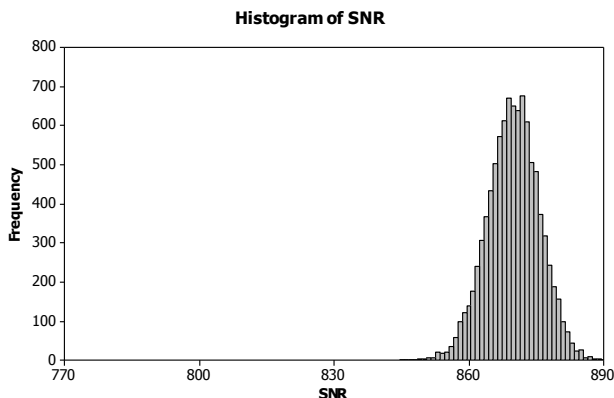


Fig. 3. Histogram of *SNR* distribution for the upper (+2 mm) surface.

An 850 *SNR* cut-off would cause the suppression of a whole point-cloud, whereas intermediate cut-off values for one plane *SNR* distributions would not suppress any single point from the other plane. This asymmetry could cause anomalous results, which suggest that, under the experimental frame of present work, *SNR* could not be used for filtering purposes.

Total distributions, on the other hand, do present clear overlapping, so it is possible to apply a filter based on this parameter. Moreover, *Total* histogram (Fig. 4) reveals a non-symmetric distribution, which complicates the calculation of cut-off values.

A statistical analysis has been performed to identify most-likely distribution. Data was fitted to a 3-Parameter Weibull distribution, in order to later establish appropriate cut-off *Total* filtering values.

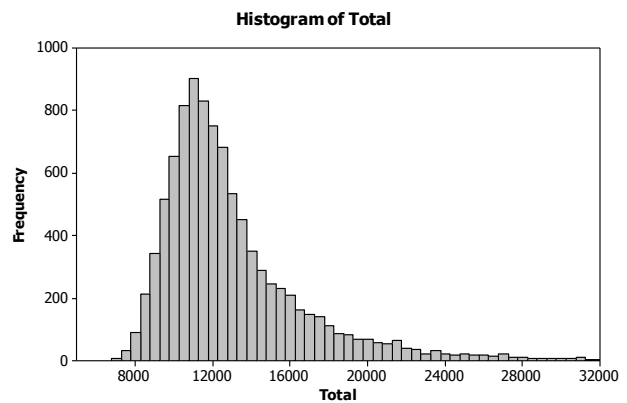


Fig. 4. Histogram of *Total* distribution for the upper (+2 mm) surface.

Finally, relative position of points with respect to the best-fit plane (Fig. 5) present a symmetric distribution with comparatively-few points concentrated on positions far away from the plane.

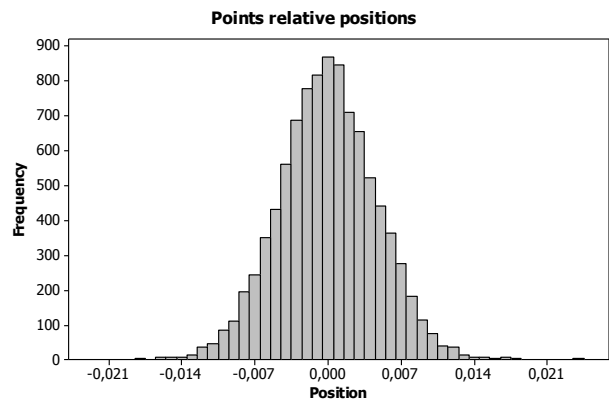


Fig. 5. Histogram of point relative position for the lower (-2 mm) surface with respect to the best-fit plane

IV. DESIGN OF EXPERIMENTS (DOE)

The DOE includes recommendations derived from preliminary test. Following this, *SNR* has been rejected as an adequate factor within the limits of this experimentation. Therefore, *Total Filter (TF)* and *Outliers Filter (OF)* were selected as factors and so does the *Order (O)* in which they are applied. Four levels were selected for *TF*: 0%; 40%; 60% and 80%. Each level represents the percentage of measurements rejected as a function of their relative distance to *Total Mode*. This reference value has been calculated during the preliminary tests based on the Weibull fitted distribution. This implies that a 40% *TF* point-cloud does only include the 60% of digitized points which *Total* values were closer to *Total Mode*. In a similar way, four levels were also considered for *OF*: 0%; 2%; 5% and 10%. This implies that a 10% *OF* point-cloud does include the 90% of digitized points which spatial positions were closer to the previously-calculated reference average position. Finally, two levels were considered for *O*: *TF* first and *OF* first. A full-factorial DOE considering 2×4^2 experiments has been thereafter defined and three replicas of each single combination have been performed where both flat surfaces have been digitized. Consequently, 96 experimental runs have provided 192 point

clouds. Each surface was represented by a 8x24 mm² region, so that an area of 192 mm² was covered on each plane. Density of points was fixed to 0.2 mm value, which means that every no-filtered point cloud contains 4,800 points. Finally, all captured point-clouds have been pre-processed to automatically reject those singular points whose positions appear to be outside the limits of WR, in order to suppress aberrant measures.

Tests were carried out during the same day in a short period of time, in order to fulfil repeatability conditions. Once the three replicas were performed, digitized point clouds were processed using specially-designed software and values for σ_d and δ_d were calculated.

V. RESULTS

A. Main Effects

TF is the main factor affecting repeatability results, as it can be clearly seen in Fig. 6. Differences in σ_d are close-to-null for the 40% filter (lower than 0.3 μm), but then suffer a rough increase to a 5.2 μm for the 80% filter. This means that repeatability nearly doubles its value when highly-restrictive filters are applied. *OF*, on the other hand, does have a reduced influence upon repeatability, since slight variations can be observed in Fig. 2. In fact, 2% filter could provide a slight improvement on repeatability values, whereas more-restrictive filters could worsen the results. Finally, although *O* presents a relative lower influence, it can be concluded that it is preferable to first apply *OF* and then apply *TF*.

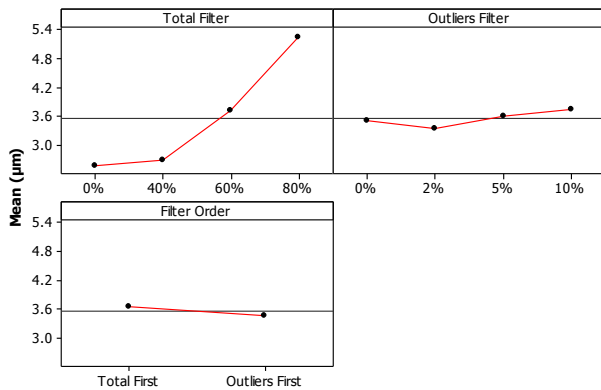


Fig. 6. Main effects plots for σ_d .

Evolution of means for δ_d can be observed in Fig. 7. It can be clearly seen that *TF* is once again the most influencing factor, while *OF* has a really low influence and *O* presents a relatively low influence. Another conclusion is that, as calculated means for this parameter always take negative values, it can be stated that, within the limits of our experimentation, conoscopic holography overestimates the distance between parallel surfaces.

Nevertheless, the effect of each single factor upon this quality indicator is completely different from that previously described for σ_d . Thus, distance values calculated using the conoscopic sensor get closer to reference values the higher the value of *TF*. Considering main effects, it can be seen how difference falls nearly a 50% (from 24.16 μm to 13.04 μm) within the limits of *TF* range.

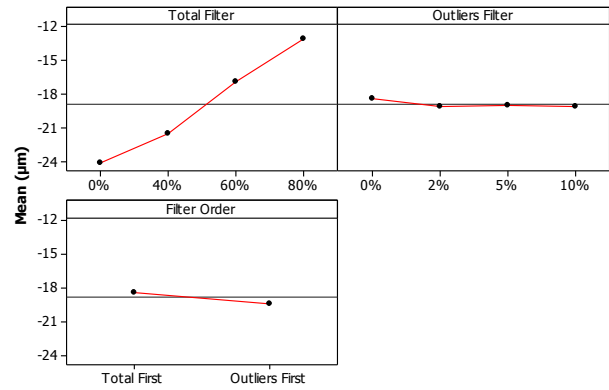


Fig. 7. Main effects plots for δ_d .

Interaction plots for σ_d (Fig. 8) allow to clarify the effect of every single factor. Interactions between the selected factors can be clearly observed, since lines present a lack of parallelism. Nevertheless, this interaction effects could have different interpretations. Thus, if analysis is limited to low 0%, 40% and 60% values for *TF* it could be concluded that no interaction occurs with *OF* as lines are parallel to each other. In a similar way, 0% and 40% *TF* do not present interaction with *O*, and also no interaction can be observed between this last factor and 0%, 2% and 5% *OF* levels. It should be remarkable that no interaction would have been observed if the most restrictive filters (80% *TF* and 10% *OF*) would have been excluded from this study. As mentioned levels are related to poorer results for σ_d it could be possible to optimize results working independently on each factor.

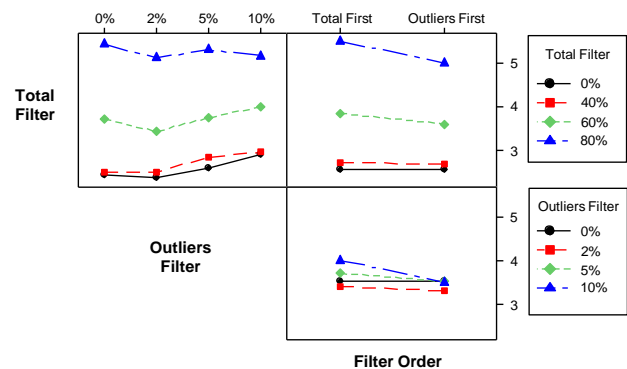


Fig. 8. Interaction plots for σ_d .

Finally, interaction plots for δ_d (Fig. 9) can be analyzed in similar terms as interaction for σ_d . Nevertheless, as it was highlighted in the analysis of main effects, factors affect trueness just in an opposite way than they affect repeatability.

This means that interaction between factors cannot be just ignored under this criterion, since it is obvious in the most restrictive filters (60% and 80% *TF*; 5% and 10% *OF*).

B. Analysis of Variance

The complex behaviour of interactions described in the previous paragraph suggests the use of an ANOVA table to obtain an improved analysis. Though this test assumes equality of variances within the populations, a Bartlett test

has been applied. This test is used to validate the hypothesis of populations having different variances thus, as p value of 0.989 for σ_d and 1.000 for δ_d have been obtained, the null hypothesis cannot be rejected. This means that data distribution does not point out to unequal variances and the ANOVA tests can be applied.

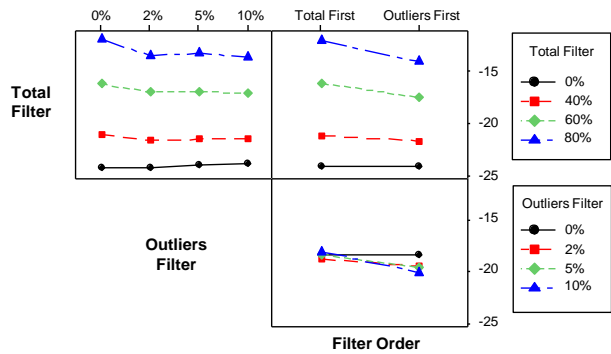


Fig. 9. Interaction plots for δ_d .

Table II contains the results for the analyses of variance for σ_d versus *Total Filter*, *Outliers Filter* and *filter Order*. Interaction of second and third order can also be found in the table.

TABLE II
ANALYSIS OF VARIANCE FOR REPEATABILITY

Source	DF	Seq SS	Adj SS	Adj MS	F	P
TF	3	110.04	110.04	36.68	167.37	0.000
OF	3	2.03	2.03	0.68	3.09	0.033
O	1	0.92	0.92	0.92	4.19	0.045
TF*OF	9	1.26	1.26	0.14	0.64	0.761
TF*O	3	0.88	0.88	0.29	1.33	0.271
OF*O	3	0.80	0.80	0.27	1.21	0.312
TF*OF*O	9	1.28	1.28	0.14	0.65	0.751
Error	64	14.03	14.03	0.22		
Total	95	131.23				

TF is confirmed as the main factor affecting repeatability, while *OF* importance is lower and *O* causes a very slight dependence. No interaction effects are really significant to a α -level of 0.05 neither for the second order ones nor for the third order interaction.

In a similar way, Table III contains the results for the analyses of variance for δ_d versus the considered factors plus the interactions.

TF is again confirmed as the main factor, whereas *O* becomes equally significant. *OF*, on the other hand, appears as a no-significant factor for trueness.

Those second order interactions which involve the *O* factor also become significant according to the ANOVA table, even when, at least for the interaction with *OF*, this significance is very slight. No significance has been found for the third order interaction.

TABLE III
ANALYSIS OF VARIANCE FOR TRUENESS

Source	DF	Seq SS	Adj SS	Adj MS	F	P
TF	3	1748.70	1748.70	582.90	361.78	0.000
OF	3	8.47	8.47	2.82	1.75	0.165
O	1	23.88	23.88	23.88	14.82	0.000
TF*OF	9	8.28	8.28	0.92	0.57	0.816
TF*O	3	14.95	14.95	4.98	3.09	0.033
OF*O	3	13.43	13.43	4.48	2.78	0.048
TF*OF*O	9	8.28	8.28	0.92	0.57	0.816
Error	64	103.12	103.12	1.61		
Total	95	1929.11				

VI. DISCUSSION

Results show that it is not possible to simultaneously optimize both σ_d and δ_d quality indicators. High values for the most significant factor (*TF*) will cause an improvement in trueness values, while simultaneously worsening repeatability values. Something similar happens with the order in which the filters are applied. Due to this situation, a decision must be taken in order to establish which the proper strategy should be.

Trueness poor values of approximately $-18 \mu\text{m}$ within the experimental range indicate a lack of accuracy in sensor performance. Nevertheless, as repeatability values are comparatively low (an average $3.56 \mu\text{m}$), accuracy could possibly be improved by introducing new features into the calibration procedure in order to compensate measurement bias. Therefore, acting upon repeatability values seems to be a better option when an optimization strategy has to be defined for improving measurement results. Accordingly, we suggest that, within the experimental conditions described above, a conservative filtering strategy should be adopted.

This strategy should consist on first applying a 2% *OF*, and the applying a 40% *TF*. The average result for repeatability value following this procedure would be approximately $2.45 \mu\text{m}$, whereas a trueness $-21.8 \mu\text{m}$ deviation would be expected.

VII. CONCLUSIONS

In this work, an analysis of filtering influence upon accuracy of CMM conoscopic holography measurements has been presented. A standard geometry formed by two parallel planar surfaces has been selected for testing purposes. Three types of filtering criteria (*SNR*, *Total* and *Outliers*) have been initially considered, while the order in which the filters should be applied has also been considered as a possible influence factor. Nevertheless, *SNR* has been lately rejected due to significant differences in each surface respective distribution for this parameters. A DOE has been therefore designed and two quality criteria regarding repeatability and trueness of measured distance between surfaces have been calculated for each single experimental run.

Experimental results have revealed that both components of accuracy: precision and trueness cannot be simultaneously

optimized under these conditions. While TF is the most important factor influencing precision and trueness, it introduces opposite effects. Recommendations have been done in order to minimize standard deviation of measurements, while compensating bias error for trueness.

Finally, results suggest that improvements in calibration procedures could be introduced in order to reduce bias error, while repeatability values could lead to consider conoscopic holography a feasible technique for quality control.

ACKNOWLEDGMENT

The authors wish to thank the ITMA Materials Technology for their help in manufacturing of the test specimen.

REFERENCES

- [1] G. Sirat and D. Psaltis, "Conoscopic holography," *Los Angeles Technical Symposium. International Society for Optics and Photonics*, 1985.
- [2] G.Y. Sirat, F. Paz, G. Agronik and K. Wilner, "Conoscopic Systems and Conoscopic Holography", *Laboratory for CAD & Lifecycle Engineering. Faculty of Mechanical Engineering, Technion-Israel Institute of Technology*, Available online: http://mecadserv1.technion.ac.il/public_html/IK05/Sirat_9375.pdf (accessed on 19 November 2013).
- [3] I. Álvarez, J.M. Enguita, M. Frade, J. Marina, and G. Ojea, "On-Line Metrology with Conoscopic Holography: Beyond Triangulation," *Sensors* 2009, 9, 7021–7037.
- [4] M. Frade, J. M. Enguita and I. Álvarez. "In situ 3D profilometry of rough objects with a lateral shearing interferometry range finder", *Optics and Lasers in Engineering*, vol. 50, Issue 11, November 2012, pp. 1559-1567.
- [5] S.L. Ko, and S.W. Park, "Development of an effective measurement system for burr geometry," *Proceedings of the Institution of Mechanical Engineers, Part B: Journal of Engineering Manufacture*, 2006, vol. 220, no 4, pp. 507-512.
- [6] L. Zhu, J. Barhak, V. Srivatsan, and R. Katz, "Efficient registration for precision inspection of free-form surfaces," *The International Journal of Advanced Manufacturing Technology*, vol. 32(5-6), pp. 505-515
- [7] R.A. Lathrop, D.M. Hackworth, and R.J. Webster III, "Minimally Invasive Holographic Surface Scanning for Soft-Tissue Image Registration," *Biomedical Engineering, IEEE Transactions on*, 2010, vol. 57, no 6, pp. 1497-1506.
- [8] G.S. Spagnolo, L. Cozzela, and C. Simonetti, "Linear conoscopic holography as aid for forensic handwriting expert," *Optik* 2013, vol. 124, pp. 2155–2160.
- [9] P. Fernández, D. Blanco, C. Rico, G. Valiño and S. Mateos, "Influence of Surface Position along the Working Range of Conoscopic Holography Sensors on Dimensional Verification of AISI 316 Wire EDM Machined Surfaces," *Sensors* 2014, vol. 14, pp. 4495-4512.
- [10] P.M. Lonardo and A.A. Bruzzone, "Measurement and Topography Characterization of Surfaces Produced by Selective Laser Sintering," *CIRP Annals–Manufacturing Technology* 2000, vol. 49, pp. 427–430.
- [11] P. Fernández, D. Blanco, G. Valiño, V. Hoang, L. Suarez and S. Mateos, "Integration of a conoscopic holography sensor on a CMM," *The 4th manufacturing engineering society international conference (MESIC 2011). AIP Conference Proceedings*, Vol. 1431, pp. 225-232 (2012)